

## Effects of *Escherichia coli* Physiology on Growth of Phage T7 In Vivo and In Silico

Lingchong You, Patrick F. Suthers, and John Yin\*

Department of Chemical Engineering, University of Wisconsin-Madison, Madison, Wisconsin 53706-1691

Received 20 September 2001/Accepted 4 January 2002

**Phage development depends not only upon phage functions but also on the physiological state of the host, characterized by levels and activities of host cellular functions. We established *Escherichia coli* at different physiological states by continuous culture under different dilution rates and then measured its production of phage T7 during a single cycle of infection. We found that the intracellular eclipse time decreased and the rise rate increased as the growth rate of the host increased. To develop mechanistic insight, we extended a computer simulation for the growth of phage T7 to account for the physiology of its host. Literature data were used to establish mathematical correlations between host resources and the host growth rate; host resources included the amount of genomic DNA, pool sizes and elongation rates of RNA polymerases and ribosomes, pool sizes of amino acids and nucleoside triphosphates, and the cell volume. The in silico (simulated) dependence of the phage intracellular rise rate on the host growth rate gave quantitatively good agreement with our in vivo results, increasing fivefold for a 2.4-fold increase in host doublings per hour, and the simulated dependence of eclipse time on growth rate agreed qualitatively, deviating by a fixed delay. When the simulation was used to numerically uncouple host resources from the host growth rate, phage growth was found to be most sensitive to the host translation machinery, specifically, the level and elongation rate of the ribosomes. Finally, the simulation was used to follow how bottlenecks to phage growth shift in response to variations in host or phage functions.**

Bacteriophage studies played a key role in setting the foundations of molecular biology (4). As a result, phage rank among the best-characterized organisms at the molecular level. Mathematical models or computer (in silico) simulations can add value to this wealth of phage information by showing how the molecular components and interactions, when taken together, can define developmental processes. For example, in recent years simulations have shown how the physicochemical interactions that govern gene regulation in lambda phage correlate with its lysis-lysogeny decision (2, 19, 22, 24), how the coupling of RNA and replicase production enables rapid takeover of the host during phage Q $\beta$  infections (10), and how the intracellular development of phage T7 depends on the organization of its genome (12, 14, 27).

The relative simplicity of phage developmental processes, compared with those of microbes or higher organisms, is balanced in part by the complexity of the resources that they need for growth. Phage require at least nucleic acid precursors, protein precursors, and translation machinery from their hosts. Consequently, phage infection processes depend not only on the physicochemical characteristics of their genome-encoded functions but also on the intracellular resources of their hosts, which depend further on the physiological state of their hosts. Studies spanning 60 years have demonstrated this dependence (1, 5–8, 11, 15, 16, 18). Different stages of phage growth, including the attachment of the phage particle to its host, the penetration of phage DNA into its host, and the synthesis of

the phage components, have been found to be sensitive to the physiological state of the host, which has been modulated by its growth medium (5, 15, 16), temperature (11, 18), oxygen tension (18), and pretreatment using chemical agents (1, 5, 15, 16). These studies have shown that the faster that the host grows at the time of phage infection, the faster that the phage will grow, corresponding to a shorter latent time (or a shorter intracellular eclipse time), faster progeny production rate, and larger burst size.

How is phage production influenced by the levels of different essential intracellular resources? The answer is not obvious because of the coupling of resources to host growth. As the growth rate of the host increases, so does its cell size (9), as well as its intracellular levels of genomic DNA, RNA polymerase, ribosomes, nucleoside triphosphates (NTPs), and amino acids (3). These are all essential resources that, to unknown extents, affect phage growth. In addition, the effects of these factors may be convoluted: the increase in the cell volume as the host cell grows faster will affect the concentrations of various resources, which in turn may affect phage growth. Mutant hosts may help uncouple these effects. For example, the effects of DNA levels can be uncoupled from growth rate by growing a *thy* mutant under thymine limitation (28). The one-step growth behavior of phage T4 on this mutant was used to infer the key role of the protein synthesis machinery in phage growth (15). Such results, while useful, do not exclude possible confounding effects of the mutation on other host resources.

Using phage T7 as the model system, we explored the effect of the host physiology on phage growth using both experimental and computational approaches. Phage one-step growth experiments were conducted by infecting *Escherichia coli* cells growing at different rates, achieved by using a chemostat.

\* Corresponding author. Mailing address: 1415 Engineering Dr., Department of Chemical Engineering, University of Wisconsin-Madison, Madison, WI 53706-1691. Phone: (608) 265-3779. Fax: (608) 262-5434. E-mail: yin@engr.wisc.edu.

TABLE 1. Dependence of *E. coli* physiological parameters on the cell growth rate ( $\mu$ , doublings per hour)<sup>a</sup>

Parameter	Equation
<i>E. coli</i> cell vol (liters).....	$V_c = 8\mu \times 10^{-16b}$
EcRNAP no. (molecules).....	$N_p = 192.2\mu^3 - 155.2\mu^2 + 549.0\mu - 103.6$
EcRNAP elongation rate (base/s).....	$k_{PE} = 108.7 - 63.6\mu^{-0.1797}$
Ribosome no. (molecules).....	$N_R = 0.8 \times (13.1\mu^2 - 6.89\mu + 6.46) \times 10^3$
Ribosome elongation rate (residue/s).....	$k_E = 102.9 - 55.5\mu^{-0.3609}$
Amino acid no. (molecules) <sup>c</sup> .....	$P = (-0.73\mu^2 + 2.74\mu + 1.48) \times 2^{(C+D)\mu/60} \times 10^{8d}$
NTP no. (molecules) <sup>c</sup> .....	$R = 1.30 P\mu/k_E$
DNA content (genome equivalent).....	$G_c = 60/(C \ln 2) [2^{(C+D)\mu/60} - 2^{\mu/60}]$

<sup>a</sup> All the equations are directly taken from reference 3 or derived from the data therein unless otherwise indicated.

<sup>b</sup> From reference 9.

<sup>c</sup> The NTP level represents the total RNA content of the host cell, and the amino acid level represents the total protein content of the host cell.

<sup>d</sup> *C* and *D* are the lengths of the *C* and *D* periods, respectively; they are related to the growth rate as follows: *C* = 42.4 + 132.7e<sup>-2.812μ</sup> (min); *D* = 22.3 + 15.4e<sup>-1.16μ</sup> (min).

These experiments suggested a similar dependence of phage growth rate on the host growth rate as observed for other phage studied: the faster that the host grows, the faster the phage infection. To better quantitatively understand this dependence, we employed a computer simulation for the intracellular growth of phage T7 in *E. coli* to probe the effect of the host physiology at the molecular level. We have previously developed a simulation to account for the mechanisms and rate of entry of the T7 DNA into the host, the transcription of the T7 genes and the translation of the resulting mRNAs, the assembly of the T7 procapsids, the replication of the T7 genome, the packaging of the new genomes into the procapsids, and the maturation of the T7 progeny (12, 13). Here we extended this simulation and explored the effects of host resources on phage growth by accounting for the coupling or uncoupling of the host resources to its growth rate.

MATERIALS AND METHODS

**Experiment. (i) Strains and growth conditions.** *E. coli* BL21 (Gal<sup>-</sup> λ<sup>s</sup> hsdS) and wild-type bacteriophage T7 were generously provided by I. J. Molineux (University of Texas, Austin). BL21 cultures were grown aerobically on Luria-Bertani (LB) broth (Difco) containing 0.4 g of glucose/liter at 30°C and pH 7 in a 3-liter KLF 2000 Fermenter (Bioengineering AG). The fermentor was inoculated with 20 ml of an overnight culture of BL21 grown on LB at 30°C. A 500 Series Fermentation Controller (Valley Instrument Co.) kept the pH, the temperature, and the impeller rotation rate (300 rpm) at set points. The feed rate to the fermentor was continuous and controlled at various rates, and the working volume was kept constant at 1,740 ml using an overflow tube. A MasterFlex pump (ColeParmer) maintained the flows in both the feed and the overflow lines. PharMed MasterFlex tubing (ColeParmer) was used for the feed and overflow tubing, CFlex tubing (ColeParmer) for the 4 N H<sub>2</sub>SO<sub>4</sub> acid and the 4 M NaOH base feeds, and platinum-cured silicone (ColeParmer) for the airflow tubing.

**(ii) Intracellular one-step growth experiments.** Established methods were used in the preparation, preservation, and assay of the phage (1, 20, 26). Bottom agar for plates and soft agar for overlayers were LB broth containing 1.5 and 0.7% Bacto agar (Difco), respectively. The host cells went through at least six to eight doublings after reaching the new steady state for each change in flow rate, as determined by optical density at 600 nm. Sampling of the chemostat was performed under sterile conditions. Ten milliliters of the sample was added to a shaker flask already at 30°C, which was then infected with phage T7. The multiplicity of infection was 0.05, and all phage growth was carried out at 30°C. At 3 min postinfection, a sample from the infected shaker flask was diluted 500-fold into 30 ml of cell-free LB medium to minimize further binding of phage to bacteria. Samples from the diluted, infected cell culture's flask were treated with chloroform (Sigma) to release intracellular phage and titered on BL21 grown in shaker flasks on LB. The number of infective centers was determined as the difference between the chloroform-treated sample and a sample that was not chloroform treated, both taken immediately after dilution. Phage dilutions for titering were performed in buffer containing 10 mM Tris-HCl (pH 7.5), 1 mM

MgCl<sub>2</sub>, 0.1 M NaCl, 10 mg of gelatin/liter, and 10 mM CaCl<sub>2</sub>. Phage growth curves were generated in triplicate at each host growth rate.

**(iii) Parameter estimation.** The objective function to extract the eclipse time, rise rate, and burst size from the intracellular one-step growth curves was defined as

$$\phi = \begin{cases} 0, & 0 < t < a \\ r(t - a), & a < t < \frac{B}{r} + a \\ B, & t > \frac{B}{r} + a \end{cases}$$

where  $\phi$  is the number of phage progeny as a function of time, *a* is the eclipse time, *r* is the rise rate, and *B* is the burst size. The nonlinear fit function of Matlab 6.0 (The Mathworks, Inc.) was used to estimate the three parameters along with their 95% confidence intervals.

**Simulation. (i) Phage T7 model.** The present T7 model, T7v2.5, recasts previous T7 models developed in our group (12, 13) using an object-oriented approach. It extends the earlier models by accounting for the stoichiometric relation of the T7 helicase/primase (gp4A) and the DNA polymerase (gp5) in forming replication complexes, or replisomes, as well as the stoichiometric balance between the number of replication complexes and the maximum number of replication forks that can form on the newly synthesized T7 genomes. In addition, it allocates *E. coli* RNA polymerases (EcRNAPs) and T7 RNA polymerases (T7RNAPs) to the synthesis of different mRNAs based on the relative strengths of the promoters. Further, it incorporates a module that facilitates the sensitivity analysis of the model with respect to single parameters or two parameters simultaneously.

While previous T7 models assumed that host resources were unbounded, the present T7 model incorporates an empirically based host cell model that accounts for experimentally observed correlations between the *E. coli* growth rate and resources such as the numbers of EcRNAP and ribosomes, the pool sizes of NTPs and amino acids, and the cell volume, shown in Table 1 and reviewed elsewhere (3). In setting up the host cell model, we treated the host cell as a spatially homogeneous resource reservoir, where the levels of the resources were defined at the initiation of the T7 infection. Moreover, by employing the equations in Table 1, we implicitly assumed the following: (i) cell volume was constant over the course of infection, (ii) there was negligible exchange of metabolites between the infected cell and its extracellular environment during infection, (iii) the model host cell represented an average of a cell population that was growing at the exponential phase immediately prior to phage infection, (iv) the initial NTP pool size was equivalent to the total RNA content of the cell, (v) NTPs were not consumed as the energy source for the reactions, and (vi) the initial amino acid pool size was equivalent to the total protein content of the cell. These assumptions were made based on our still limited understanding of the interplay between phage T7 and its *E. coli* host; some of them are open to debate. For example, as detailed in Discussion, the value for the NTP pool size was chosen mainly because of the lack of mechanistic understanding on the exact level of NTP in the host cell that is available for phage development. Nevertheless, these assumptions serve as a starting point toward representing the host cell, and they can be refined when more experimental data and mechanisms become available.

Compared with its precursor simulations, T7v2.5 is significantly improved in

several aspects. First, with an object-oriented design, T7v2.5 presents a framework that can be easily generalized to model the growth of other kinds of viruses. Second, by incorporating a host cell model and updating the mechanisms of several viral infection steps, T7v2.5 gives overall better agreement with the experiments for the base simulation, particularly in the prediction of the intracellular rise rate (27). Third, the computation speed of T7v2.5 is more than 10-fold higher than that of its direct precursor, T7v2 (12). The source code of T7v2.5 is available on request.

(ii) **Computer simulations.** We performed a sensitivity analysis on all the *E. coli* physiological parameters that affect the growth of T7 (Table 1). Here we use the term “sensitivity analysis” in its broad sense, i.e., the determination of changes in the value of model variables in responding to the change in a parameter value. The base case value of the host growth rate was set to 1.5 doublings/h, and the corresponding base case values of the other parameters were calculated using the equations in Table 1. In each sensitivity analysis, one parameter was varied over a range from 0.1 to 10 times its base case value, while the other parameters were kept constant, and a simulation was conducted for each value of the selected parameter. For scenarios where host physiology was defined by a single growth rate, we coupled host resources to the growth rate using the equations in Table 1. To provide a basis for comparison with the experiments we conducted, the host growth rate was varied from 0.7 to 1.7 doublings per h. Each simulation was conducted over a period of 60 min with a time step of 0.02 s for numerical integration, except for those where the host cell volume was less than half its base case value. In this case, a time step of 0.001 s was used to avoid computational errors resulting from the integration of stiff equations (e.g., the assembly of procapsid is 4.8th order in terms of the concentration of major capsid protein; significant computational errors may occur when this concentration is high, which may arise for small volumes and large time steps). The sensitivity of phage growth to both EcRNAP and ribosomes was studied by generating a mesh of 400 (or 20 by 20) nodes ranging from 0.1- to 100-fold of the base case values, and the rise rate was determined at each node. Derivatives with respect to EcRNAP number and ribosome number were then determined at each node, and local changes in these derivatives were used to demark transitions in resource limitation. Specifically, the boundary between the EcRNAP-limited growth and ribosome-limited growth was defined between nodes where the derivative of the rise rate with respect to the EcRNAP numbers changed from positive to either negative or zero. Further, the boundary between growth limitations by protein synthesis and DNA synthesis was defined between nodes where the derivative of the rise rate with respect to both EcRNAP numbers and ribosome numbers changed from positive to either negative or zero.

## RESULTS

**T7 growth was sensitive to *E. coli* growth rate.** The host *E. coli* cell can affect phage T7 growth in many ways. From the perspective of the intracellular processes comprising the phage infection cycle, the *E. coli* cell serves at least as a set of material resources. Additionally, the cell volume may affect viral growth by affecting the concentrations of interacting molecular species. The physiological parameters that characterize the levels of these cellular resources and the cell volume are all closely correlated with the cell growth rate (3). Therefore, changes in the cell growth rate will change the physiological parameters; in turn, these changes may affect the rate of phage development. We found from our experiments and simulations that phage infections indeed became increasingly productive as the growth rate of the host *E. coli* increased from 0.7 to 1.7 doublings per h (Fig. 1).

To better compare simulations and experiments, we characterize each intracellular one-step growth curve using three variables: the time required by the infected host to produce the first phage progeny (eclipse time), the rate of intracellular phage progeny production (rise rate), and the total number of viable progeny per infected host (burst size), as shown in Fig. 2A. Since the mechanism for the phage-induced lysis of the host cell is not well understood and not included in our simulation, we focus here on the behaviors of the eclipse time and

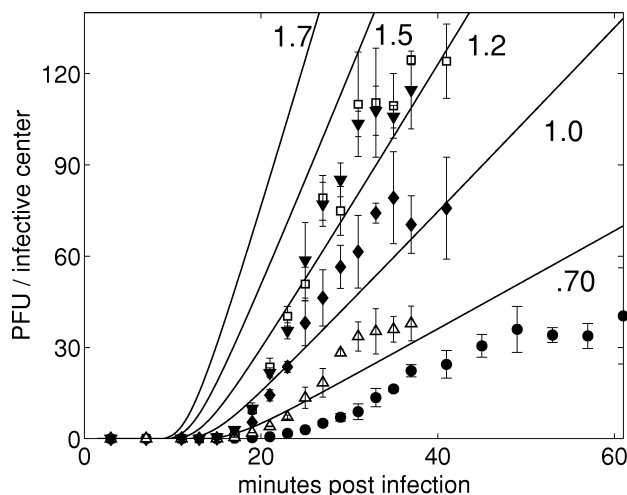


FIG. 1. Intracellular one-step growth of phage T7 on *E. coli* BL21 growing at different rates. The host cells were grown at 0.7, 1.0, 1.2, 1.5, and 1.7 doublings per h. Experimental data of the intracellular PFU for each host growth rate are from three separate infections indicated by black circles, white triangles, black diamonds, black triangles, white squares, in the order of the growth rates above; Bars indicate standard deviations. Output from the simulation is shown by solid lines.

the rise rate, which are lysis insensitive. The simulation agreed well with experiments in predicting the dependence of the eclipse time and the rise rate on the *E. coli* growth rate (Fig. 2B and C): the rise rate monotonically increased and the eclipse time monotonically decreased with increasing *E. coli* growth rates. The agreement for the rise rate was better overall than for the eclipse time, where there was a systematic mismatch between simulation and experiment (Fig. 2C, solid line). Also note from Fig. 2 that the rise rate was much more sensitive to the changes in the *E. coli* growth rate than was the eclipse time. As the *E. coli* growth rate increased from 0.7 to 1.7 doublings per h, the rise rate increased approximately fivefold, whereas the eclipse time decreased by less than 30%. This sensitivity analysis gives an overall picture of the dependence of T7 growth on the *E. coli* physiological state.

**Simulated T7 growth most strongly depended on the number and the elongation rate of ribosomes.** To investigate *in silico* the effect of individual *E. coli* physiological parameters on T7 growth, we uncoupled them from the *E. coli* growth rate and from each other and analyzed the sensitivity of the rise rate and the eclipse time to each, independently. As in the case of the sensitivity analysis on the *E. coli* growth rate (Fig. 2B and C), the rise rate was overall much more sensitive to the host parameter changes than was the eclipse time. In addition, the rise rate and the eclipse time always changed in inverse directions with any parameter changes; therefore, we focus here on the rise rate.

The number and the elongation rate of ribosomes had the strongest effect on the rise rate (Fig. 3). They had virtually the same effect until they were large, where the rise rate leveled off at different levels. The increase in ribosome elongation rates increased the rise rate more than did the increase in the ribosome numbers. The dependence of the rise rate on the cell volume was overall moderate and, interestingly, biphasic; the rise rate first increased and then decreased as the cell volume

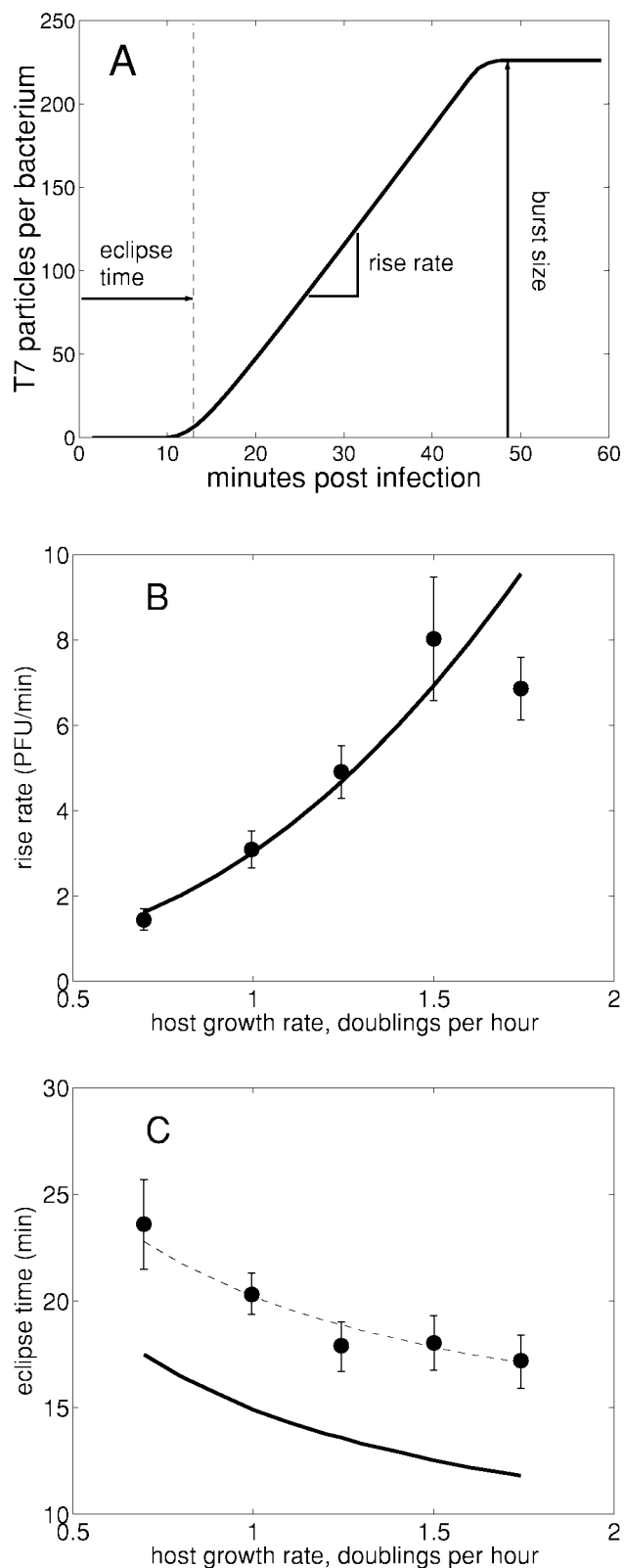


FIG. 2. Phage T7 growth dependence on host growth rate. (A) An intracellular one-step growth curve can be characterized by three variables: eclipse time is the period between infection initiation and the time point when phage progeny first appear, the rise rate is the slope of the straight line starting from the end of the eclipse period, and the burst size is the final number of phage progeny produced from a single

increased from 0.1 to 10 times its base case value (Fig. 3). The optimal rise rate occurred at the base case cell volume.

The dependence of T7 growth on the other host parameters was less significant (Fig. 3). An increase in the DNA content had a slightly positive effect on the rise rate. The amino acid pool size did not have any significant effect on the rise rate until it was smaller than about 0.25 times its base case value, when the rise rate became sensitive to the parameter: as the amino acid pool size dropped from 0.25 to 0.1 times its base case value, the rise rate decreased from close to its base case value to nearly zero. The number and the elongation rate of EcRNAPs had similar effects on T7 growth within the range of parameter values examined: the rise rate decreased to a similar degree as either increased (Fig. 3). In the range of parameter values examined, the variation in the NTP pool size did not have any effect on the rise rate (data not shown).

To better understand how an increase in the EcRNAP number could slow down T7 growth, we examined the effect of the increase in the EcRNAP number on the production of several phage components. We found that, with the other parameters kept constant at their base case values, an increase in the EcRNAP number reduced the rate of procapsid synthesis (Fig. 4A). This reduction corresponded with significant increases in the number of ribosomes allocated to the mRNAs for the early T7 genes, such as 0.7 (T7 kinase gene) and 1 (T7RNAP gene), and reductions in the number of ribosomes allocated to the mRNAs for the late T7 genes, such as 9 (scaffold protein gene), 10A (major capsid protein gene), and 19 (DNA maturation protein gene) (Fig. 4B).

### DISCUSSION

We employed experiments and computer simulations of the phage T7 intracellular growth cycle to investigate how the host physiological conditions affect phage growth. Although previous studies have shifted host physiologies in shaker cultures by using media based on different carbon sources (15), we found that chemostat cultures using constant growth media but different dilution rates yielded greater flexibility, control, and reproducibility of results. Further, by using chemostat-cultured hosts for our one-step growth studies, we provided a better basis for comparison with our simulations, which employed host resource parameters measured from continuous cultures (Table 1).

Consistent with our experimental results, the simulations predicted that faster-growing host cells supported faster T7 growth (Fig. 1 and 2B and C). The simulations give overall better predictions on the rise rate than on the eclipse time. The systematic mismatch between predicted and experimental values for eclipse time (Fig. 2C) may result from the instantaneous nature of several “hard-switches” that we implement in

infection. (B) The intracellular rise rate; (C) the eclipse time. Both are extracted using a three-parameter model from the data in Fig. 1, as a function of the *E. coli* growth rate. The experimental results are shown in black circles, and 95% confidence intervals are indicated. Results of processing the computer simulation growth curves are shown by solid lines. A one-parameter adjustment to the eclipse time is shown by a dashed line. This adjustment incorporated a constant delay in the initiation of phage adsorption to the host cell.

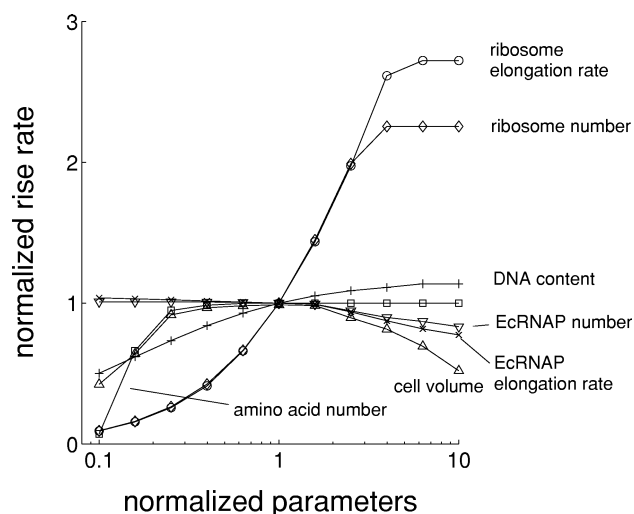


FIG. 3. Sensitivity of the intracellular rise rate to host physiological parameters. The parameters were normalized to their base case values, which were calculated based on an *E. coli* growth rate of 1.5 doublings per h using equations from Table 1. The rise rate was normalized to the value calculated from the base case parameters. Because the NTP number did not affect the rise rate over the parameter range examined, it is omitted from the figure.

the simulation, where data or mechanisms are not available. These switches include the initiation of phage DNA entry, the initiation of T7RNAP-modulated translocation and transcription, and the initiation of host DNA digestion. For instance, we assume a 90-s delay for the initiation of phage adsorption, which can take longer. Increasing this delay by 5.3 min can eliminate the mismatch (Fig. 2C, dashed line). Nonetheless, this correction does not exclude potential contributions from other factors. Although the intracellular one-step growth curves cannot distinguish between these mechanisms, available experimental data on the intracellular processes of T7 infection at the molecular level may provide some hints. A close examination of earlier data on T7 protein expression (14) suggests that the mismatch is unlikely due to a delay in phage absorption because T7 proteins begin to appear around 2 min after infection. Further, since expression of class II proteins initiates in less than 2 min after the appearance of T7RNAPs (14), the second mechanism cannot completely account for the mismatch either. The last mechanism seems to contribute the major part of this mismatch. In fact, we assumed that the host DNA is digested between 7.5 and 15 min after infection. These time points were based on experiments that measured the degradation of host DNA by T7 infection at 37°C (23) and could be significantly delayed at 30°C, the temperature used in the present study. Similar experiments conducted at 30°C will help to explain the mismatch and improve the simulation by providing more accurate parameters.

Previous efforts to identify key host constraints to phage growth have been hindered by the experimental challenge of independently modulating and studying the effects of different host resources on phage growth (15, 16). We have addressed this challenge by using the simulation to numerically uncouple the host intracellular resources from the host growth rate and

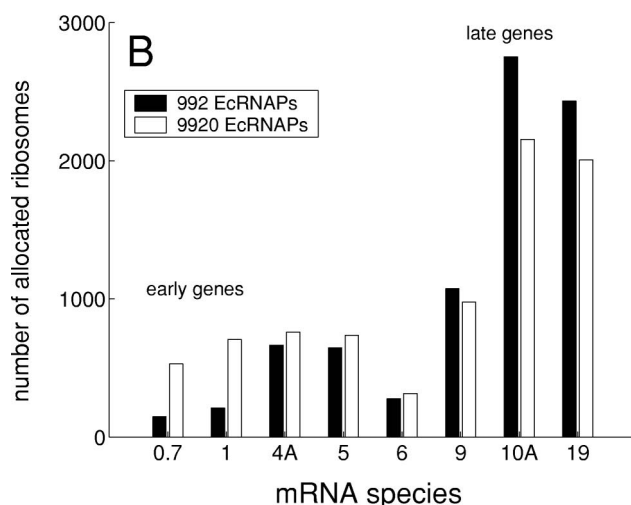
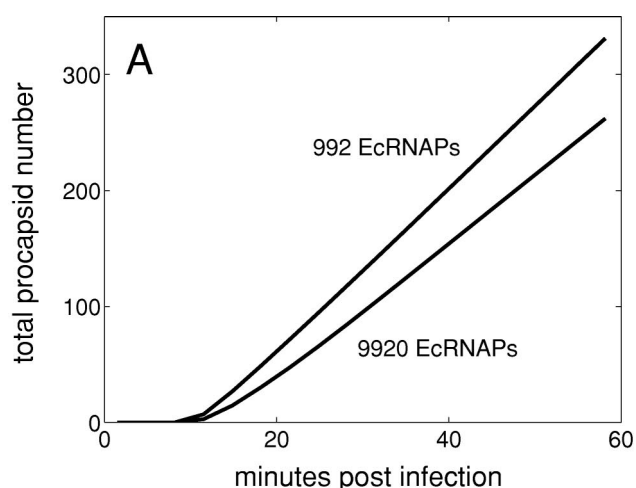


FIG. 4. Effect of the EcRNAP number on the procapsid assembly process (A) and the allocation of ribosomes to different mRNAs (B) (a snapshot taken at 21 min post-infection initiation). The total procapsid number accounts for both mature capsids and procapsids.

then independently examine their effects on phage growth. While such studies may appear to distort relationships among the host resources, they are useful for two reasons. First, they allow us to better understand how uncertainties in parameters may affect the behavior of the simulation. While empirically determined cell compositions and activities are well defined, it is not always clear what may be accessible for phage growth. For example, NTP pool size in the simulation is based on the total host cell RNA content, which includes both stable and unstable RNAs (3). However, we do not know for certain what fraction of the total NTPs per cell is accessible to T7 processes during infection. On the one hand, since stable RNAs constitute parts of ribosomes that are needed by T7 for protein translation, they are improbable precursors for producing T7 mRNAs. On the other hand, the unstable RNAs alone are probably inadequate to support phage growth. Further, the host cell may have means of providing NTPs for phage growth,

for example, by continuing to synthesize NTPs during infection; to our knowledge there has been no evidence that T7 infection shuts down host NTP synthesis. Because of the resultant uncertainty in the accessible NTP pool size, it is useful to explore the effects on phage growth of a broad range of values. Second, studying the sensitivity of the simulated phage growth to extreme changes in single-host parameters may reveal aspects of phage development in cells growing in complex environments or in highly distorted hosts like anucleate minicells (21). By varying host growth rates in a chemostat, we have considered only a narrow range of conceivable host resource distributions. Hosts growing in complex environments, where spatial gradients and dynamic variations in nutrients, temperatures, and pH can be significant, may well have intracellular resource distributions that drastically differ from our experiments. While we lack detailed information about how resources might be correlated in these cases, determining the sensitivity of phage growth to variations in single or paired host parameters can begin to provide insights into potential constraints under such conditions.

The sensitivity analysis with the individual host physiological parameters indicates that T7 growth most strongly depends on the number and the elongation rate of the ribosomes, suggesting that the rate-limiting step of phage growth is the synthesis of phage proteins. However, since the ribosome elongation rate only increases slightly as the cell growth rate increases, its contribution is probably less important than the ribosome number, which increases much more rapidly with the cell growth rate (Table 1). Thus, our simulation results support the hypothesis that the amount per cell of the host translation machinery is one of the most crucial factors in determining the rate of phage growth (15). This result is also consistent with the weaker dependence of phage growth on the number and elongation rate of EcRNAPs, the sizes of the NTP and amino acid pools, and the DNA content, although all these factors also play indispensable roles during T7 growth.

Because of the complex nature of the viral infection dynamics, increasing the amount of an essential component may actually slow down viral growth, as demonstrated by the counterintuitive observation that an increase in the EcRNAP number can decrease the T7 growth rate (Fig. 3). One may expect that increasing the EcRNAP number would increase mRNA levels, protein synthesis rates, and finally the T7 growth rate. This expectation holds when the EcRNAP number is sufficiently small or when the ribosome number is sufficiently high (data not shown). In either scenario, T7 growth is limited by transcription and this limitation can be relieved by an increase in the EcRNAP number. When the EcRNAP number is too large, however, T7 growth will be limited by translation. In this case, increasing the number of EcRNAPs, which are mainly responsible for the transcription of T7 class I genes, will result in a higher level of early mRNAs and divert the ribosomes away from the translation of several late proteins that are needed in large quantities for phage particle formation (Fig. 4B), particularly the scaffold protein (gp9) and the major capsid protein (gp10A). gp10A is especially important for two reasons: first, compared with other T7 proteins, it is needed in the largest quantity for each T7 particle (25); second, the rate of procapsid assembly is assumed to be proportional to  $[gp10A]^{4.8}$  (12, 13). Hence, even a slight decrease in gp10A

level may significantly decrease the procapsid assembly rate (Fig. 4A) and in turn significantly decrease the rise rate. In summary, when translation is already limited by the ribosome number, an increase in EcRNAP number causes ribosomes to distribute in a manner that is unfavorable for the expression of important late proteins, thus reducing the rise rate (Fig. 3).

Our simulations indicate that T7 growth is more sensitive to the processivity of T7RNAPs than to the processivity of EcRNAPs, although the effect of either factor is much weaker than that of the ribosomes (data not shown). This is to be expected because the transcription of T7 genes is primarily dependent on T7RNAP, which is more efficient than EcRNAP in internalizing and transcribing T7 DNA. This point further suggests that T7 growth limitation by the host translation machinery may well be because the phage provides its own highly efficient RNA polymerase, thus creating a bottleneck for processing of its mRNAs.

The biphasic effect of the cell volume on T7 growth is another demonstration of the complexity of the infection dynamics. A large cell volume may slow down the intracellular interactions by causing a decrease in the concentrations of interacting species. This is particularly true for the assembly of procapsids from major capsid proteins (gp10A). An increase in the cell volume can result in a decrease in the gp10A concentration, which in turn can cause a major decrease in the procapsid assembly rate. When the cell volume is too small, however, other effects may dominate: the inhibition of EcRNAP by gp0.7 and gp2 and the inhibition of T7RNAP by gp3.5 will be enhanced because of the increased total concentrations for these proteins. Consequently, under such conditions fewer free T7RNAP and EcRNAP molecules are available for the transcription of viral genes and the rate of viral protein expression decreases, which in turn reduces the rate of phage progeny formation. This idea is supported by the observation that the numbers of active EcRNAPs and T7RNAPs decrease with a decreasing cell volume (data not shown). In summary, extremes in cell volume can, through different mechanisms, have detrimental effects on T7 growth.

As the activity of host or phage functions vary, so too may that of bottlenecks to phage production, as shown in the "bottleneck landscape" of Fig. 5. For the base case parameters, T7 growth is bottlenecked or limited by the rate of protein synthesis, which is determined by the level of ribosomes. If one relieves this bottleneck by increasing the ribosome number, then the phage growth becomes limited by the host transcription rate, determined by the level of EcRNAP. When levels of both ribosomes and EcRNAPs are high, then the bottleneck to phage growth can become the rate of its own DNA synthesis. While such a scenario may be unlikely for wild-type phage growth on a wild-type host, due to the >10-fold increases that would be required for both the EcRNAP and ribosome levels, phage mutants that expressed reduced DNA synthetic capacities could alter the landscape by expanding the DNA synthesis-limiting region. In summary, specific features of the bottleneck landscape will change with genetic or environmental modifications to phage or host functions, but so long as the simulation accounts for the modifications, the corresponding landscapes can be created.

Although simulations can facilitate the analysis of complex processes like the growth of phage T7 in its host cell, what the

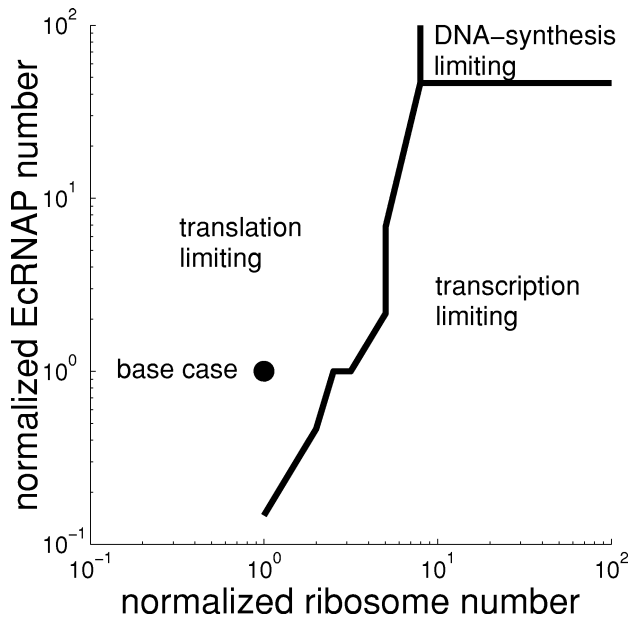


FIG. 5. A “bottleneck landscape” for phage T7 growth with respect to two host parameters, the levels of the host RNA polymerase (EcRNAP) and ribosome. At any point on this figure, phage growth is limited by the rate of translation by the host ribosomes or of transcription by the EcRNAP or of phage DNA synthesis. The base case setting is labeled by the filled circle.

results of simulations truly reflect is the behavior of the model. How well the model predictions apply to the real system depends on the accuracy and completeness of the knowledge base and the validity of the simplifying assumptions implemented in the model. The knowledge base in turn has been accumulated and will be enriched through continued laboratory experiments. To this end, simulations may facilitate the learning process by revealing key deficiencies or inconsistencies in the knowledge base and by making experimentally testable predictions. For example, the prediction that the rate of T7 growth was limited primarily by the synthesis of the late proteins, especially the major capsid protein (gp10A), could be tested by designing specialized ribosomes (17) that preferentially translated gp10A mRNA. If the simulation is correct, then enhanced expression of gp10A should increase the rate of T7 progeny formation. If experimental results do not match the prediction, then the mismatch serves as a foundation for refining the model. It is the iterative experimental testing and refinement of simulation by experiments that gradually promote a systems-level integration of data and that ultimately aim to shed light on relationships otherwise difficult to observe.

#### ACKNOWLEDGMENTS

We thank Jeremy Francken and William Wodicka for their technical assistance and Ranjan Srivastava for reading and commenting on the manuscript. We also thank Ian J. Molineux for helpful discussions, and two anonymous reviewers for their comments and suggestions.

This work was supported by the Office of Naval Research (grant no. N00014-98-1-0226), the National Science Foundation Presidential Early Career Award to J.Y. (grant no. BES-9896067), and Merck Research Laboratories. P.F.S. was supported by a National Science Foundation Graduate Fellowship.

#### REFERENCES

- Adams, M. H. 1959. Bacteriophages. Interscience, New York, N.Y.
- Arkin, A., J. Ross, and H. H. McAdams. 1998. Stochastic kinetic analysis of developmental pathway bifurcation in phage lambda-infected *Escherichia coli* cells. *Genetics* **149**:1633–1648.
- Bremer, H., and P. P. Dennis. 1996. Modulation of chemical composition and other parameters of the cell by growth rate, p. 1553–1569. *In* F. C. Neidhardt, R. Curtiss III, J. L. Ingraham, E. C. C. Lin, K. B. Low, B. Magasanik, W. S. Reznikoff, M. Riley, M. Schaechter, and H. E. Umbarger (ed.), *Escherichia coli* and *Salmonella*: cellular and molecular biology, 2nd ed., vol. 2. ASM Press, Washington, D.C.
- Cairns, J., G. S. Stent, and J. D. Watson. (ed.) 1992. Phage and the origins of molecular biology. Cold Spring Harbor Laboratory Press, Plainview, N.Y.
- Cohen, S. S. 1949. Growth requirements of bacterial viruses. *Bacteriol. Rev.* **13**:1–24.
- Cohen, S. S. 1953. Studies on controlling mechanisms in the metabolism of virus-infected bacteria. *Cold Spring Harbor Symp. Quant. Biol.* **18**:221–235.
- Cohen, S. S. 1947. The synthesis of bacterial viruses in infected cells. *Cold Spring Harbor Symp. Quant. Biol.* **12**:35–49.
- Delbrück, M. 1946. Bacterial viruses or bacteriophages. *Biol. Rev. Camb. Philos. Soc.* **21**:30–40.
- Donachie, W. D., and A. C. Robinson. 1987. Cell division: parameter values and the process, p. 1578–1593. *In* F. C. Neidhardt, J. L. Ingraham, K. B. Low, B. Magasanik, M. Schaechter, and H. E. Umbarger (ed.), *Escherichia coli* and *Salmonella typhimurium*: cellular and molecular biology, vol. 2. American Society for Microbiology, Washington, D.C.
- Eigen, M., C. K. Biebricher, M. Gebinoga, and W. C. Gardiner. 1991. The hypercycle. Coupling of RNA and protein biosynthesis in the infection cycle of an RNA bacteriophage. *Biochemistry* **30**:11005–11018.
- Ellis, E. L., and M. Delbrück. 1939. The growth of bacteriophage. *J. Gen. Physiol.* **22**:365.
- Endy, D. 1997. Ph.D. thesis. Dartmouth College, Hanover, N.H.
- Endy, D., D. Kong, and J. Yin. 1997. Intracellular kinetics of a growing virus: a genetically structured simulation for bacteriophage T7. *Biotechnol. Bioeng.* **55**:375–389.
- Endy, D., L. You, J. Yin, and I. J. Molineux. 2000. Computation, prediction, and experimental tests of fitness for bacteriophage T7 mutants with permuted genomes. *Proc. Natl. Acad. Sci. USA* **97**:5375–5380.
- Hadas, H., M. Einav, I. Fishov, and A. Zaritsky. 1997. Bacteriophage T4 development depends on the physiology of its host *Escherichia coli*. *Microbiology* **254**:179–185.
- Hedén, C.-G. 1951. Studies of the infection of *E. coli* B with the bacteriophage T2. *Acta Pathol. Microbiol. Scand. Suppl.* **89**.
- Hui, A., and H. A. de Boer. 1987. Specialized ribosome system: preferential translation of a single mRNA species by a subpopulation of mutated ribosomes in *Escherichia coli*. *Proc. Natl. Acad. Sci. USA* **84**:4762–4766.
- Kutter, E., E. Kellenberger, K. Carlson, S. Eddy, J. Neitel, L. Messinger, J. North, and B. Guttman. 1994. Effects of bacterial growth conditions and physiology on T4 infection, p. 406–418. *In* J. D. Karam (ed.), *Molecular biology of bacteriophage T4*. ASM Press, Washington, D.C.
- McAdams, H. H., and L. Shapiro. 1995. Circuit simulation of genetic networks. *Science* **269**:650–656.
- Miller, J. H. 1992. A short course in bacterial genetics. A laboratory manual and handbook for *Escherichia coli* and related bacteria. Cold Spring Harbor Laboratory Press, Cold Spring Harbor, N.Y.
- Ponta, H., J. N. Reeve, M. Pfennig-Yeh, M. Hirsch-Kauffmann, M. Schweiger, and P. Herlich. 1977. Productive T7 infection of *Escherichia coli* F+ cells and anucleate minicells. *Nature* **269**:440–442.
- Reinitz, J., and J. R. Vaisnys. 1990. Theoretical and experimental analysis of the phage lambda genetic switch implies missing levels of co-operativity. *J. Theor. Biol.* **145**:295–318.
- Sadowski, P. D., and C. Kerr. 1970. Degradation of *Escherichia coli* B deoxyribonucleic acid after infection with deoxyribonucleic acid-defective amber mutants of bacteriophage T7. *J. Virol.* **6**:149–155.
- Shea, M. A., and G. K. Ackers. 1985. The O<sub>R</sub> control system of bacteriophage lambda. A physical-chemical model for gene regulation. *J. Mol. Biol.* **181**:211–230.
- Steven, A. C., and B. L. Trus. 1986. The structure of bacteriophage T7, p. 1–35. *In* J. R. Harris and R. W. Horne (ed.), *Electron microscopy of proteins*, vol. 5. Academic Press, London, United Kingdom.
- Studier, F. W. 1969. The genetics and physics of bacteriophage T7. *Virology* **39**:562–574.
- You, L., and J. Yin. 2001. Simulating the growth of viruses. *Pac. Symp. Biocomput.* **2001**:532–543.
- Zaritsky, A., and C. L. Woldring. 1973. Changes in cell size and shape associated with changes in the replication time of the chromosome of *Escherichia coli*. *J. Bacteriol.* **114**:824–837.